Biol Cybern (2015) 109:321–332
DOI 10.1007/s00422-015-0645-7

ORIGINAL PAPER

Biological Cybernetics

Continuous neural network with windowed Hebbian learning

M. Fotouhi · M. Heidari · M. Sharifitabar

Received: 25 November 2013 / Accepted: 27 January 2015 / Published online: 13 February 2015

Abstract We introduce an extension of the classical neural field equation where the dynamics of the synaptic kernel satisfies the standard Hebbian type of learning (synaptic plasticity). Here, a continuous network in which changes in the weight kernel occurs in a specified time window is considered. A novelty of this model is that it admits synaptic weight decrease as well as the usual weight increase resulting from correlated activity. The resulting equation leads to a delay-type rate model for which the existence and stability of solutions such as the rest state, bumps, and traveling fronts are investigated. Some relations between the length of the time window and the bump width is derived. In addition, the effect of the delay parameter on the stability of solutions is shown. Also numerical simulations for solutions and their stability are presented.

Keywords Neural field · Continuous network · Bump · Traveling front · Delay equation · Existence · Stability

Mathematics Subject Classification 35B35 · 35C07 · 45K05 · 92B20 · 92C20

M. Fotouhi
Department of Mathematical Sciences, Sharif University of Technology, P.O. Box 11365-9415, Tehran, Iran
e-mail: fotouhi@sharif.edu

M. Heidari
Department of Mechanical Engineering, Sharif University of Technology, P.O. Box 11155-9567, Tehran, Iran
e-mail: maziar_heidari@mech.sharif.ir

M. Fotouhi · M. Heidari · M. Sharifitabar (✉)
School of Mathematics, Institute for Research in Fundamental Sciences (IPM), P.O. Box 19395-5746, Tehran, Iran
e-mail: mohsen@sharifitabar.com

1 Introduction

Recent advances in brain imaging has made a significant progress in observing the dynamics of neural populations. This makes the study of activity patterns in large networks a challenging task (see for example [3,6,7,9,10]). So far one of the best models of choice at the level of large neural populations is the classical neural field equations. Having proposed the classical neural fields, Wilson and Cowan [34,35] have numerically shown some solutions such as solitary bumps. This model is simplified to a single layer of neurons by Amari [2] where analytical solutions for bump states were obtained. Since the simplified model was analytically tractable, the existence and stability of many solutions were determined.

The classical neural field with static kernel is obtained by the general formula

$$\tau \partial_t u(x,t) = -u(x,t) + \int_{\mathbb{R}} w(x,y) f(u(y,t))\,\mathrm{d}y, \qquad (1)$$

where $u(x,t)$ represents the local activity of a population of neurons at position x and time t. Also $f(u)$ denotes the firing rate function, and it is taken to be Heaviside or a sigmoid function. The coupling function $w(x,y)$ represents the connection weights between neuron's population at x and y and is often assumed to be homogeneous so that $w(x,y) = w(x-y)$. There have been several types of solutions suggested for the above formulation (1) such as standing bump solution in which a region of the network is activated, and wave-like solutions (traveling fronts, spiral and breathing waves, traveling bumps) which propagate through the neural network [11,12,14,21,23,28]. Another important solution for such models is the rest state solution, i.e., equal activity for all neurons. Moreover, the stability of the rest

case $u(x,t) = 0$ in Eq. (1) is important due to the possible presence of some perturbation.

A more challenging task, however, would be to consider the behavior of large neural systems in the face of changing dynamics of neural connectivity.

There is a vast literature on learning dynamics many of which are related to spiking neurons as well as rate models. Here, a possible extension of the classical neural field model is to make room for a Hebbian type of synaptic modification [20]. Many variants of the Hebbian learning explain the nature of neural representation and its relation to the coding mechanisms observed in biological neural tissue [15,26].

One of general mathematical formulation of the synaptic efficacy dynamics between neuron i and j which is suggested by Gerstner and Kistler [17] has the following relation

$$\frac{\mathrm{d}}{\mathrm{d}t} w_{ij} = F\left(w_{ij}; v_i, v_j\right), \tag{2}$$

where w_{ij} is the synaptic connectivity weight between neurons i and j at time t. The variables v_i and v_j stand for the firing rates of the neurons i and j, respectively. The function F represents the dynamics functionality of the learning process.

Some variants of Hebbian type of synaptic modification such as BCM and Oja's rule and others is extensively discussed in neural modeling literature [1,4,25,29,32]. The simplest choice for the learning function which relies on the correlation-based Hebbian learning rule has the following form for a positive function $c = c(w_{ij})$,

$$\frac{\mathrm{d}}{\mathrm{d}t} w_{ij} = c v_i v_j. \tag{3}$$

Thus, if neurons i and j have the same spiking activities, the synaptic efficacy connecting these neurons, w_{ij}, will be strengthened. There are restricting rules imposed on the functionality selection of F as listed below (see [13,17]).

1. There should be the locality of the dynamics which means that the dynamics of the synaptic strength between neurons i and j is only dependent upon the characteristics of neurons i and j and independent of all other neurons.
2. The type of synaptic connections is invariant in the learning process. Namely, the excitatory synaptic connections do not change into inhibitory connections and vice versa.
3. The stability of such dynamics requires a maximum and minimum values for the synaptic strength so the function F should contain a term which determines upper and lower bounds of w_{ij} [4,24]. For instance, if the parameter c in Eq. (3) tends to zero as w_{ij} approaches its maximum value, a saturation of synaptic weights can be achieved (see [17]). Then for example $c = \gamma(w_{\max} - w_{ij})$ in Eq. (3) ensures the boundedness of the synaptic strength.
4. Hebbs original proposal does not contain a rule for a decrease of synaptic weights. In a system where synapses can only be strengthened, all efficacies will finally saturate at their upper maximum value. An option for decreasing the weights is therefore a necessary requirement for a realistic learning (plasticity) rule, since by applying only the Hebbian learning, the synaptic strength only tends to increase. This can, for example, be achieved by weight decay, which can be implemented in Eq. (3) by subtracting the term μw_{ij} (see [16]),

$$\frac{\mathrm{d}}{\mathrm{d}t} w_{ij} = -\mu w_{ij} + c v_i v_j. \tag{4}$$

In this paper, we shall address a basic question in computational neuroscience as to how to extend the classical neural field equation with synaptic dynamics without sacrificing the basic dynamical constraints such as boundedness and synaptic decay.

Although in principle, many of the well-known spike or rate-based learning rules may be extended to a neural field formulation, this is not mathematically always easy to do. So for example in the case of Spike-Timing-Dependent-Plasticity, it is not clear how to track the order of spikes even in the case of a rate model (see [30]). However, for a simple correlation-based type of learning such as the Hebbian, the intuition of neurons that fire together wire together, carries over to the neural field formulation in an obvious way. A correlated increase in activity will cause the strengthening of the corresponding connections between the two locations. At the very basic level, this strengthening of connectivity may stabilize solutions such as bumps of activity which otherwise would lose stability due to noise or inhomogeneity in the network. The former is exemplified in the recent work [3] where it is shown that due to the destabilizing effect of noise, correlated activity will not last for too long. In the latter case of inhomogeneity, the possible drift of any bump solution has nicely been shown by Itskov et al. [22]. Based on their results, synaptic plasticity helps to stabilize the bumps for an appropriate time, relevant to the behavioral level of activity.

Before we get into the specifics of the network dynamics, two important aspects of the Hebbian extension need to be considered. First, we need to ensure the boundedness of the synaptic kernel [4,24] and second, to make it more realistic, we shall let the strength of the connections to decay when the activation becomes less correlated [13,17].

Now in its most general form, one may consider a synaptic dynamics where the correlated-based plasticity is a history-based rule (see for example [33]) rather than being dependent on the instantaneous value of the neuron's activity. In other words, studying population dynamics at the macro level, where points in close proximity will strengthen their connections based on the past and present join activation, the

synaptic dynamics may be regarded as a continuous process throughout the whole continuum. The constraints mentioned above lead to the following type of an extended continuous network equation,

$$\begin{aligned}\tau\,\partial_t u(x,t) &= -u(x,t) + \int_{\mathbb{R}} w(x,y,t)\,f(u(y,t))\,\mathrm{d}y,\\ \partial_t w(x,y,t) &= \gamma(w_m(x,y) - w(x,y,t))\,f(u(x,t))\,f(u(y,t)),\end{aligned} \tag{5}$$

where $w_m(x,y)$ is a maximum value of each synaptic connection $w(x,y,t)$ and it is assumed to be in a homogeneous form $w_m(x-y)$. Also if we consider the homogeneous case for the initial value of the synaptic weight,

$$w(x,y,0) = (1-\kappa)w_m(x-y), \quad 0<\kappa<1,$$

the solution of Eq. (5) will be

$$w(x,y,t) = w_m(x-y) \times \left(1-\kappa\exp\left(-\gamma\int_0^t f(u(x,s))\,f(u(y,s))\,\mathrm{d}s\right)\right).$$

The integral term in the above relation can be interpreted as correlation between firing rates of the neurons positioned at x and y in the time interval $[0,t]$.

The above model has a slight disadvantage: no unlearning rule is contained. One can overcome this by applying a decay in the weights. But here we propose a more intrinsic rule to obtain this. The idea is that it is not necessary to increase constantly the strength of the connection between two neurons which are fired together for a long period of time. Also it seems reasonable to decrease the connection strength between two neurons which were correlated in the past, but not correlated in the present time. One of the most simple models, which captures these ideas, is to use a delay-type equation,

$$\begin{aligned}\partial_t w(x,y,t) = \gamma(w_m - w)\Big[&f(u(x,t))\,f(u(y,t)) \\ &- f(u(x,t-\delta))\,f(u(y,t-\delta))\Big].\end{aligned} \tag{6}$$

This new model involves the history of the activity of network and current activity has some trace in the future of the network. We also may rewrite this equation in an integral form,

$$w(x,y,t) = w_m(x-y) \times \left(1-\kappa\exp\left(-\gamma\int_{t-\delta}^t f(u(x,s))\,f(u(y,s))\,\mathrm{d}s\right)\right).$$

We may interpret this integral form as considering the correlation over a time window of length δ. As can be seen in the present model, both the boundedness of synaptic strength as well as synaptic weakening holds.

Here, the change in the weight kernel at time t depends on the time window δ before t. This has the novel advantage of studying δ as a bifurcation parameter and analyzing its effect on the stability of the solutions. We end up with the following continuous network with a delay dynamics for synaptic weight connections,

$$\begin{cases}\tau\,\partial_t u(x,t) = -u(x,t) + \displaystyle\int_{\mathbb{R}} w(x,y,t)\,f(u(y,t))\,\mathrm{d}y,\\ w(x,y,t) = w_m(x-y) \\ \quad\times\left(1-\kappa\exp\left(-\gamma\int_{t-\delta}^t f(u(x,s))\,f(u(y,s))\,\mathrm{d}s\right)\right).\end{cases} \tag{7}$$

In this paper, we consider the above model and investigate the existence and stability of solutions such as rest state, bumps and traveling fronts. In addition, the effect of time window length δ as a bifurcation parameter is shown on the stability of these types of solutions.

2 Constant steady states

In this section, we investigate the constant steady-state solutions and their stability. A constant steady-state solution is a time-independent and spatially uniform solution, i.e., $u(x,t) = \overline{u}$ interpreted as a rest state of the network, especially the zero solution $u(x,t) = 0$.

2.1 Existence

Let $u(x,t) = \overline{u}$ be a constant steady state of the system (7). It follows that,

$$\begin{cases}\overline{w}(x,y) = \left(1-\kappa\mathrm{e}^{-\gamma\delta f(\overline{u})^2}\right)w_m(x-y),\\ \overline{u} = \left(1-\kappa\mathrm{e}^{-\gamma\delta f(\overline{u})^2}\right)W f(\overline{u}),\\ W = \displaystyle\int_{\mathbb{R}} w_m(y)\,\mathrm{d}y.\end{cases} \tag{8}$$

In the case of Mexican-hat kernel $w_m(x) = \frac{1}{4}(1-|x|)\mathrm{e}^{-|x|}$, one calculates $W=0$ and we have the unique steady-state solution $\bar{u}=0$. If we consider the sigmoid firing rate function $f(u) = 1/(1+\mathrm{e}^{-\beta(u-h)})$, we always have at least a steady-state solution (not necessarily unique) and this is shown in Fig. 1 for the exponential kernel $w_m(x) = \frac{1}{2}\mathrm{e}^{-|x|}$.

2.2 Stability

For the investigation of stability, we linearize the system (7) around the rest solution,

$$\begin{cases}\tau\,\partial_t v = -v + \displaystyle\int_{\mathbb{R}}\left(\omega(x,y,t)\,f(\overline{u}) + \overline{w}(x,y)\,f'(\overline{u})\,v(y,t)\right)\mathrm{d}y,\\ \omega(x,y,t) = \kappa\gamma\,w_m(x-y)\,f(\overline{u})\,f'(\overline{u})\mathrm{e}^{-\gamma\delta f(\overline{u})^2} \\ \quad\times\int_{t-\delta}^t (v(x,s)+v(y,s))\,\mathrm{d}s.\end{cases}$$

Let $\alpha = \kappa e^{-\gamma\delta f(\overline{u})^2}$. Therefore,

$$\tau\partial_t v = -v + \alpha\gamma f(\overline{u})^2 f'(\overline{u}) \int_{t-\delta}^{t} \big(W v(\cdot, s) + w_m * v(\cdot, s)\big)\, \mathrm{d}s + (1-\alpha) f'(\overline{u})(w_m * v).$$

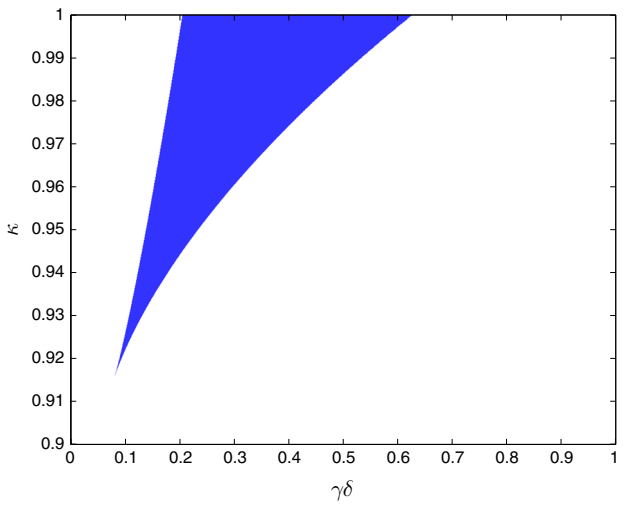

Fig. 1 The stability criterion for the exponential kernel in accordance with the Eqs. (8) and (10). In the colored area, we have at least one unstable constant solution. The other parameters are $\beta = 25$, $h = 0.05$ and $W = 1$

Letting the solution to be of the form $v(t, x) = e^{\lambda t} v(x)$, we obtain the characteristic equation for the spectral values,

$$\tau\lambda v = -v + \alpha\gamma f(\overline{u})^2 f'(\overline{u}) \frac{1 - e^{-\delta\lambda}}{\lambda} (W v + w_m * v) + (1-\alpha) f'(\overline{u})(w_m * v).$$

Taking Fourier transform yields,

$$\tau\lambda + 1 - (1-\alpha) f'(\overline{u}) \widehat{w}_m(\xi) - \alpha\gamma f(\overline{u})^2 f'(\overline{u})(W + \widehat{w}_m(\xi)) \frac{1 - e^{-\delta\lambda}}{\lambda} = 0, \tag{9}$$

for some $\xi \in \mathbb{R}$. The following theorem shows the stability condition for the rest state solution in two cases of Mexican-hat kernel and an excitatory network. In both cases, synaptic weight kernel is symmetric and $W + \widehat{w}_m(\xi) \geq 0$ everywhere. You can find the proof of the following theorem in Appendix.

Theorem 1 *In the case of an excitatory network, the steady-state solution $u = \overline{u}$ is stable if and only if,*

$$\left(1 - \kappa e^{-\gamma\delta f(\overline{u})^2} \left(1 - 2\gamma\delta f(\overline{u})^2\right)\right) f'(\overline{u}) W < 1. \tag{10}$$

This condition is automatically true for the extreme possible values of $\overline{u}$. Considering Mexican-hat weight function, the stability condition for $\overline{u} = 0$ is

$$\left(1 - \kappa e^{-\gamma\delta f(0)^2} \left(1 - \gamma\delta f(0)^2\right)\right) f'(0) < 4. \tag{11}$$

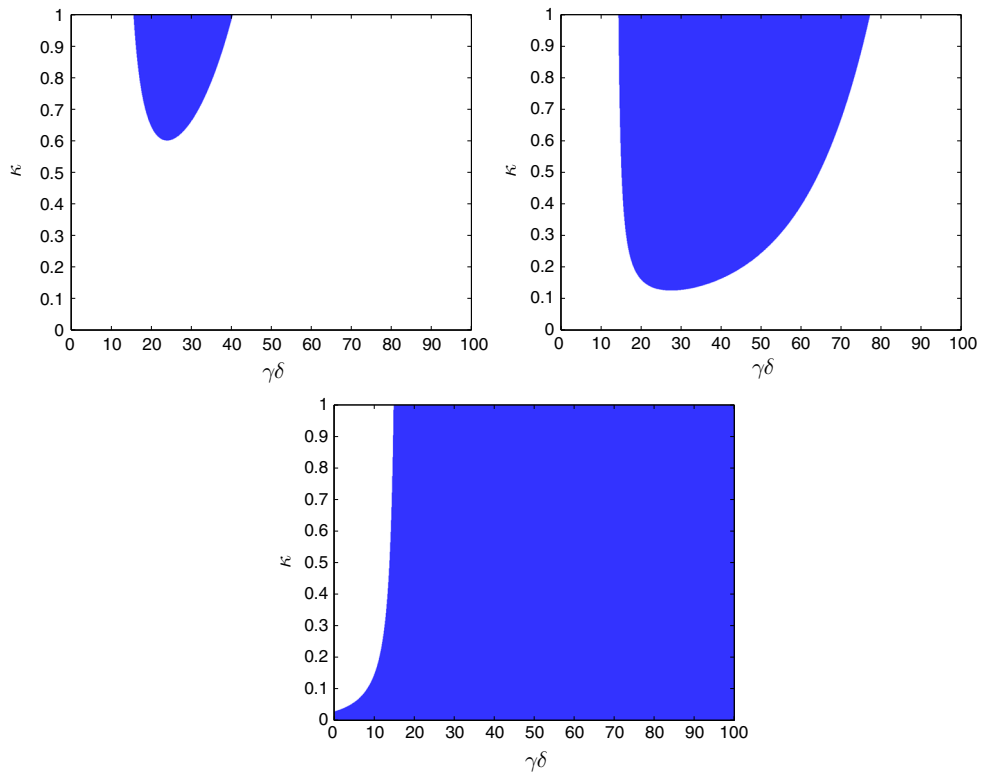

Fig. 2 The instability region of the solution $u = 0$ for the Mexican-hat kernel. We take $h = 0.05$ and $\beta = 18, 20, 22$, respectively

Remark 2 As we can see in the proof of this theorem, in the unstable cases, for every value of ξ, the characteristic Eq. (9) has exactly one root in $\mathrm{Re}\lambda \geq 0$ corresponds to the eigenfunction $v(x) = \exp(\mathrm{i}\xi x)$. Indeed, with the increase of $\widehat{w}_m(\xi)$, the value of the root λ of Eq. (9) will be increased. Therefore, the intersection of spectrum and the right half-plane is exactly the interval $[0, \lambda_M]$ where λ_M is the eigenvalue corresponds to the maximum value of $\widehat{w}_m(\xi)$ and the corresponding value of ξ is the dominant mode of instability.

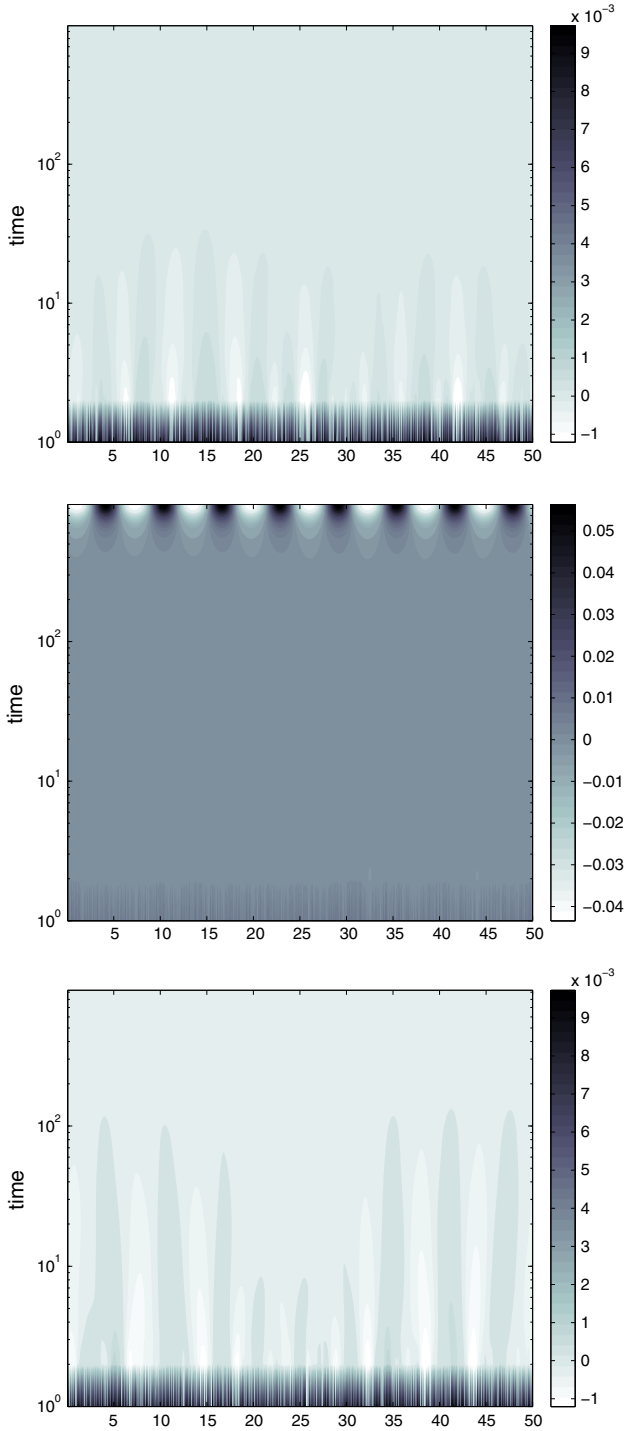

Fig. 3 Spatio-temporal dynamics of the rest-state solution of Mexican-hat kernel for the values of $\delta = 10, 40, 70$ from *top* to *bottom*. The parameters are $\kappa = 0.3$, $h = 0.05$, $\beta = 20$ and $\gamma = 1$. The time axes are in log scale for better appearing

The existence and stability conditions of rest-state solutions in the case of exponential kernel are plotted in Fig. 1. It might be seen that for these set of parameters, if the capacity κ is large enough, there exist a range of $\gamma\delta$ in which we have at least one unstable constant solution. For the only constant solution $\overline{u} = 0$ in the case of Mexican-hat kernel, its instability region which is determined by Eq. (11) is plotted in Fig. 2. We can see that this condition might be very sensitive to the sigmoid function parameter β.

The simulation results of the rest-state which has the Mexican-hat kernel for three values of δ (chosen from stable and unstable regions) are plotted in Fig. 3. A positive noisy perturbation of amplitude 0.01 at time $t = 0$ is applied to a periodic domain of length $L = 50$ and we run the simulations until $t = 1{,}000$. As it is depicted, the rest state is stable for the case of $\delta = 10$ and $\delta = 70$, whereas it is unstable for the case of $\delta = 40$ and in this case, a strip pattern emerges which corresponds to the dominant mode $\exp(\mathrm{i}x)$ according to Remark 2. It is worth-mentioning that this pattern appears regardless of the initial perturbation.

3 One-bump solutions

A stationary pulse solution known as bump activity is a class of solutions in the continuous networks. Since in the mechanism of short-term memory, some part of the prefrontal cortex is activated, the stationary pulse solutions are related to temporary storage of information within the brain [18]. Having been disconnected from external stimulus, the cortical memory neurons are persistent to establish a representation of the stimulus. In the following, we analytically study the bump solutions in the network equipped with the Heaviside firing rate function and the Hebbian learning. The analysis is somehow difficult for the sigmoid firing rate, so we restrict our attention to the limiting case, i.e., Heaviside function.

3.1 Existence

Let $f(u) = H(u - h)$ and let $u(x, t) = b(x)$ be a one-bump solution with radius a, i.e., $b(x) > h$ if and only if $|x| < a$. We must have the following equalities,

$$\begin{cases} b(x) = w_b * f(b), \\ w_b(x, y) = w_m(x - y)\left(1 - \kappa \mathrm{e}^{-\gamma\delta f(b(x)) f(b(y))}\right). \end{cases}$$

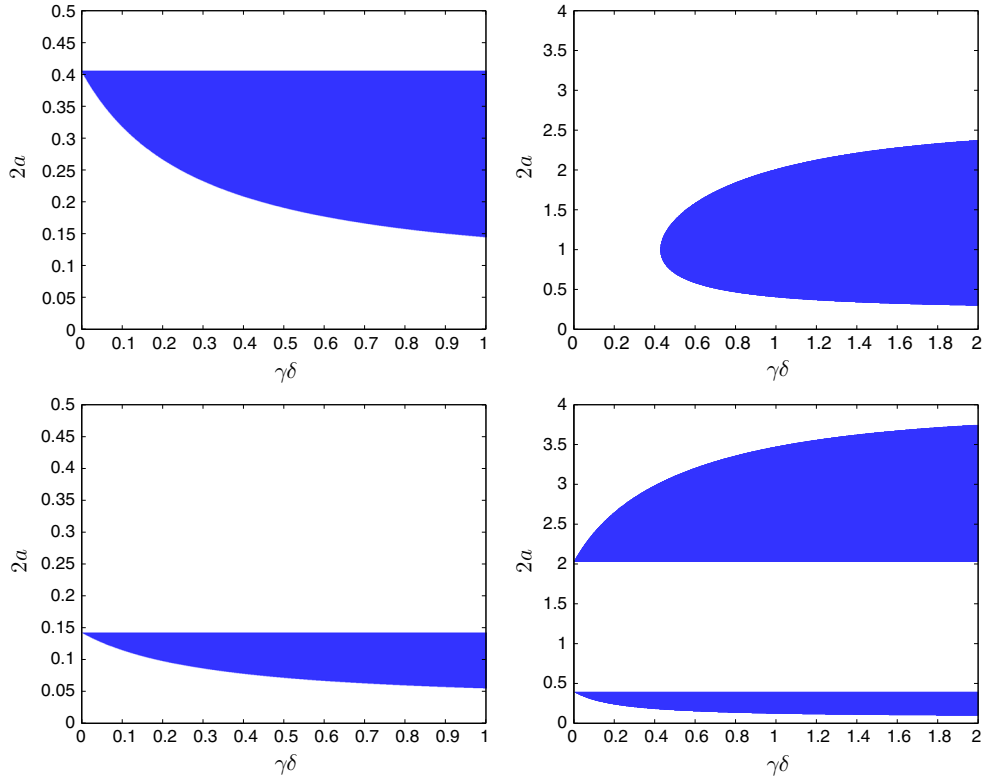

Fig. 4 Possible values of bump width with respect to the delay parameter for the exponential (*left*) and Mexican-hat (*right*) kernel. The parameters are $\kappa = 0.7$ and $h = 0.05$ (*top*) and $h = 0.02$ (*bottom*)

Therefore,

$$b(x) = \int_{-a}^{a} w_b(x, y)\,\mathrm{d}y = \left(1 - \kappa \mathrm{e}^{-\gamma\delta f(b(x))}\right) \int_{-a}^{a} w_m(x - y)\,\mathrm{d}y.$$

Hence,

$$b(x) = \begin{cases} (1-\kappa) \displaystyle\int_{-a}^{a} w_m(x-y)\,\mathrm{d}y, & |x| > a, \\ \left(1 - \kappa \mathrm{e}^{-\gamma\delta}\right) \displaystyle\int_{-a}^{a} w_m(x-y)\,\mathrm{d}y, & |x| < a. \end{cases} \tag{12}$$

Note that according to the above relations, there is no continuous bump solution. However, we can consider the solution of Eq. (7), in the space of piecewise continuous functions. So we need the condition

$$b_+(a) \le h \le b_-(a),$$

where $+$ and $-$ signs mean the right and left limit of function b at point a, respectively. Then, we can find a necessary and sufficient condition for the existence of such bump,

$$\frac{h}{1 - \kappa \mathrm{e}^{-\gamma\delta}} \le \int_0^{2a} w_m(y)\,\mathrm{d}y \le \frac{h}{1-\kappa}. \tag{13}$$

Figure 4 shows the regions for which a bump of width $2a$ exists. We see that as we expected, by increasing the delay, we have more bumps. It is interesting that for the Mexican-hat kernel, we have no bump solution for small values of delay parameter.

3.2 Stability

Here, we formally linearize Eq. (7) around the bump solution $b(x)$ with radius a. The analysis is not rigorous, but we will see in simulations that such a result could be true.

$$\begin{aligned} \tau \partial_t v = &-v + \int_{\mathbb{R}} w_b(x, y) f'(b(y)) v(y, t)\,\mathrm{d}y \\ &+ \kappa\gamma \mathrm{e}^{-\gamma\delta f(b(x))} \int_{\mathbb{R}} w_m(x - y) f(b(y)) \\ &\int_{t-\delta}^{t} \Big(v(x, s) f'(b(x)) f(b(y)) \\ &+ v(y, s) f'(b(y)) f(b(x)) \Big)\,\mathrm{d}s\,\mathrm{d}y. \end{aligned}$$

Let the solution to be of the form $v(x, t) = \mathrm{e}^{\lambda t} v(x)$. So we obtain the characteristic equation for the spectral values,

$$(\tau\lambda+1)v(x)=\int_{\mathbb{R}} w_b(x,y)f'(b(y))v(y)\,\mathrm{d}y +\kappa\gamma\frac{1-\mathrm{e}^{-\delta\lambda}}{\lambda}\mathrm{e}^{-\gamma\delta f(b(x))} \times\int_{\mathbb{R}} w_m(x-y)f(b(y)) \times\Big(v(x)f'(b(x))f(b(y)) +v(y)f'(b(y))f(b(x))\Big)\,\mathrm{d}y. \tag{14}$$

We use the relation

$$\int f'(b(x))u(x)\mathrm{d}x=\sum_{b_\pm(z)=h}\frac{u_\pm(z)}{|b'_\pm(z)|},$$

to simplify Eq. (14) which is valid for continuous b without the $\pm$ signs. Note that because of the discontinuity of b at the points where it is equal to the threshold h, only one of the $+$ and $-$ signs (right and left limit, respectively) are acceptable at each point.

We can consider three kinds of bump solutions. First, the case that the both inequalities in (13) are strict. In this case, the bump is obviously stable, because $f'(b(x))=0$ for every x, and we arrive at the eigenvalue equation $(\tau\lambda+1)v(x)=0$. Second, the case $h=(1-\kappa)\int_0^{2a}w_m(y)\,\mathrm{d}y$, where the bumps satisfy $b_+(a)=h<b_-(a)$.

$$(\tau\lambda+1)v(x)=w_{b+}(x,a)\frac{v_+(a)}{|b'_+(a)|}+w_{b-}(x,-a)\frac{v_-(-a)}{|b'_-(-a)|} +\kappa\gamma\frac{1-\mathrm{e}^{-\delta\lambda}}{\lambda}\mathrm{e}^{-\gamma\delta f(b(x))}v(x)f' \times(b(x))\int_{-a}^{a}w_m(x-y)\,\mathrm{d}y.$$

If we rewrite the above relation for the limited cases $x\to a^+$ and $x\to -a^-$, we achieve the Evans function (see [31]),

$$(\tau\lambda+1)v_+(a)=(1-\kappa)\left(w_m(0)\frac{v_+(a)}{|b'_+(a)|} +w_m(2a)\frac{v_-(-a)}{|b'_-(-a)|}\right),$$
$$(\tau\lambda+1)v_-(-a)=(1-\kappa)\left(w_m(2a)\frac{v_+(a)}{|b'_+(a)|} +w_m(0)\frac{v_-(-a)}{|b'_-(-a)|}\right).$$

Note that $|b'_+(a)|=|b'_-(-a)|=(1-\kappa)|w_m(0)-w_m(2a)|$, so

$$\tau\lambda=\frac{w_m(0)\pm w_m(2a)}{|w_m(0)-w_m(2a)|}-1. \tag{15}$$

Hence assuming $w_m(0)>0$, for stability we must have $w_m(2a)<0$.

Finally, the third case of the bumps is the case $h=(1-\kappa\mathrm{e}^{-\gamma\delta})\int_0^{2a}w_m(y)\,\mathrm{d}y$, which the bumps satisfy $b_+(a)<h=b_-(a)$. Similarly, we have the eigenvalue equation,

$$(\tau\lambda+1)v(x)=w_{b-}(x,a)\frac{v_-(a)}{|b'_-(a)|}+w_{b+}(x,-a)\frac{v_+(-a)}{|b'_+(-a)|} +\kappa\gamma\frac{1-\mathrm{e}^{-\delta\lambda}}{\lambda}\mathrm{e}^{-\gamma\delta f(b(x))} \times\left(v(x)f'(b(x))\int_{-a}^{a}w_m(x-y)\,\mathrm{d}y +f(b(x))\left(w_m(x-a)\frac{v_-(a)}{|b'_-(a)|} +w_m(x+a)\frac{v_+(-a)}{|b'_+(-a)|}\right)\right),$$

and Evans function obtained by $x\to a^-$ and $x\to -a^+$,

$$(\tau\lambda+1)v_-(a)=\left(1+\kappa\mathrm{e}^{-\gamma\delta}\left(\gamma\frac{1-\mathrm{e}^{-\delta\lambda}}{\lambda}-1\right)\right) \times\left(w_m(0)\frac{v_-(a)}{|b'_-(a)|}+w_m(2a)\frac{v_+(-a)}{|b'_+(-a)|}\right),$$
$$(\tau\lambda+1)v_+(-a)=\left(1+\kappa\mathrm{e}^{-\gamma\delta}\left(\gamma\frac{1-\mathrm{e}^{-\delta\lambda}}{\lambda}-1\right)\right) \times\left(w_m(2a)\frac{v_-(a)}{|b'_-(a)|}+w_m(0)\frac{v_+(-a)}{|b'_+(-a)|}\right).$$

Here, $|b'_-(a)|=|b'_+(-a)|=(1-\kappa\mathrm{e}^{-\gamma\delta})|w_m(0)-w_m(2a)|$, so

$$(1-\kappa\mathrm{e}^{-\gamma\delta})(\tau\lambda+1)=\Big(1+\kappa\mathrm{e}^{-\gamma\delta} \times\left(\gamma\frac{1-\mathrm{e}^{-\delta\lambda}}{\lambda}-1\right)\Big)\frac{w_m(0)\pm w_m(2a)}{|w_m(0)-w_m(2a)|}. \tag{16}$$

Conjecture 3 *The bump solution in the case* $h=(1-\kappa)\int_0^{2a}w_m(y)\,\mathrm{d}y$ *is stable if and only if* $w_m(2a)<0$. *The case* $h=(1-\kappa\mathrm{e}^{-\gamma\delta})\int_0^{2a}w_m(y)\,\mathrm{d}y$ *is stable if and only if* $w_m(2a)<0$ *and,*

$$\frac{w_m(0)+w_m(2a)}{w_m(0)-w_m(2a)}<\frac{1-\kappa\mathrm{e}^{-\gamma\delta}}{1-(1-\gamma\delta)\kappa\mathrm{e}^{-\gamma\delta}}. \tag{17}$$

So a bump in the case of an excitatory network is unstable near the threshold values of a.

For the second part, we use the following argument. Let $A=1-\kappa\mathrm{e}^{-\gamma\delta}$ and $B=\dfrac{w_m(0)\pm w_m(2a)}{|w_m(0)-w_m(2a)|}$, then rewrite Eq. (16) as the following,

$$\frac{A}{B}(\tau\lambda+1)-A-\gamma(1-A)\frac{1-\mathrm{e}^{-\delta\lambda}}{\lambda}=0. \tag{18}$$

Similar to the proof of Theorem 1, we show that in (18), if $\mathrm{Re}\lambda\geq 0$, we must have $\mathrm{Im}\lambda=0$. Otherwise, assume that

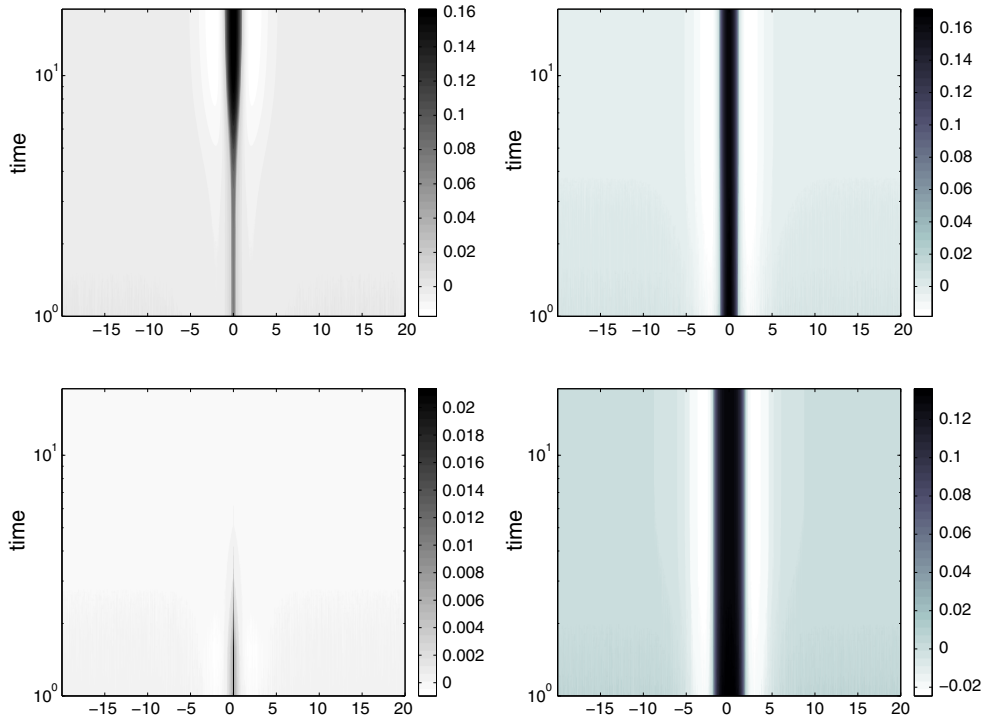

Fig. 5 The time evolution of the bumps with radius $a = 0.1982$ (*top left*), 1.0148 (*top right*), 0.0487 (*bottom left*) and 1.8736 (*bottom right*). We can see these values in Fig. 4. The parameters are $\kappa = 0.7$, $h = 0.02$, $\delta = 2$ and $\gamma = 1$. The time axes are in log scale for better appearing

$\lambda = r + \mathrm{i}m$ and $m \neq 0$ and $r \geq 0$. Considering imaginary parts,

$$0 = \frac{A}{B}\tau(r^2 + m^2) + \gamma(1 - A) \times \left(1 - \mathrm{e}^{-\delta r}\cos(m\delta) + r\mathrm{e}^{-\delta r}\frac{\sin(m\delta)}{m}\right) \geq \gamma(1 - A)\left(1 - \mathrm{e}^{-\delta r} - r\delta\mathrm{e}^{-\delta r}\right) > 0,$$

which is a contradiction. Note that $0 < A < 1$ and $0 < B$ in both Mexican-hat kernel or excitatory network cases.

Now consider Eq. (18) on $[0, \infty)$, and note that its left-hand side is an increasing function of λ, so it will have a positive real root if and only if its value at $\lambda = 0$ is negative. Therefore, the condition of stability is,

$$\frac{A}{B} - (A + \gamma\delta(1 - A)) > 0.$$

Note that we implicitly assume that $w_m(0) > 0$.

The simulations of one-bump solutions for $h = 0.02$ are utilized in Fig. 5 for the threshold values to verify the stability results. The top diagrams corresponds to the case $h = (1 - \kappa)\int_0^{2a} w_m(y)\,\mathrm{d}y$, and the bottom diagrams corresponds to the other case. According to Conjecture 3, the left ones should be unstable and the right ones should be stable. We run the simulations in a periodic domain of length $L = 40$ until $t = 20$. Again at $t = 0$, we apply a positive noise of amplitude 0.01 in stable cases and 0.001 in unstable cases. In bottom left, the bump disappear after some time, but in the top left, the solution converges to another wider bump which is stable. In fact it seems that wider bumps are more stable.

Also we do the simulations in the case of sigmoid firing rate function, as you can see in Fig. 6. We use an iteration to find the bump as a fixed point, starting from the solution we obtained by Heaviside function. For small values of β, this iteration does not converge to a one-bump solution and we do not know if such a solution exist. Here for $\beta = 100$, the bump is not stable and two bumps appear near the original bump. But the bump is stable for larger values of β, like the Heaviside firing rate.

Also, coming back to Heaviside firing rate function, we may analyze the effect of parameter δ on the stability of bumps. Again according to Conjecture 3, the case $h = (1 - \kappa)\int_0^{2a} w_m(y)\,\mathrm{d}y$ is unstable for a range of parameter δ, but it is stable for small enough and large enough values of δ. We can see the validity of these results in Fig. 7. Again as in the stability region of constant steady state, the results is hugely sensitive to sigmoid parameter, if we use a sigmoid firing rate function instead. For example, these stabilities are not true anymore even if we take a sigmoid function with parameter $\beta < 2{,}000$. This is a remarkable fact, as it shows

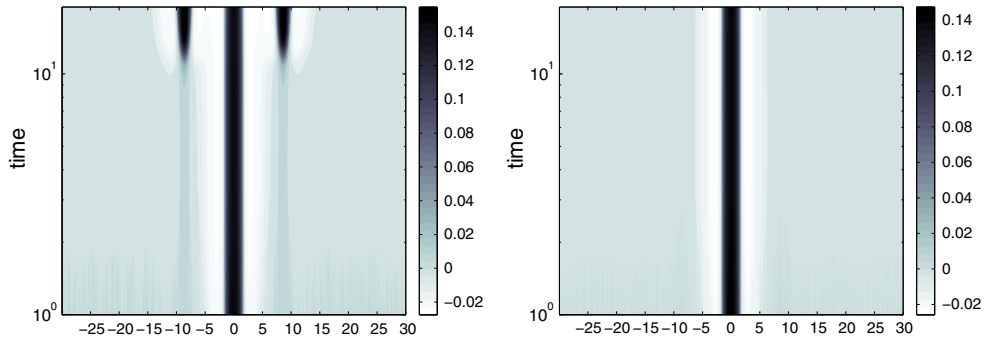

Fig. 6 The time evolution of the bumps with radius $a = 0.1982$, but this time with a sigmoid firing rate function with parameters $\beta = 100$ (*left*) and $\beta = 105$ (*right*). The other parameters are $\kappa = 0.7$, $h = 0.02$, $\delta = 2$ and $\gamma = 1$. The time axes are in log scale for better appearing

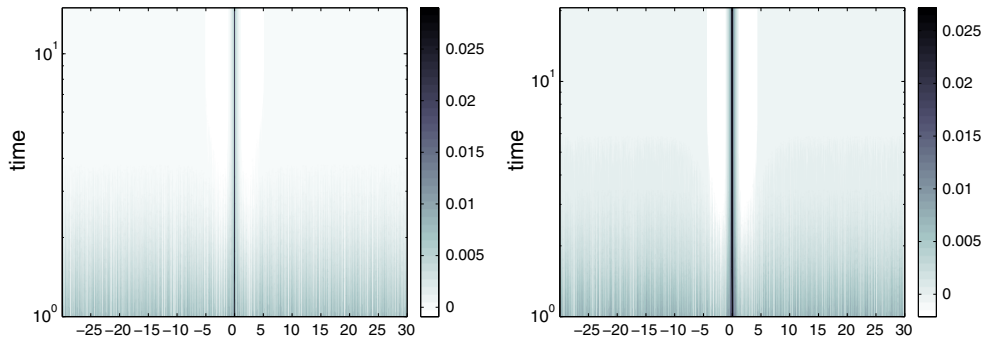

Fig. 7 The time evolution of the bumps with radius $a = 0.0437$, $\delta = 6.0$ (*left*), and $a = 0.0903$, $\delta = 0.4$ (*right*). The parameters are $\kappa = 0.7$, $h = 0.02$ and $\gamma = 1$. The time axes are in log scale for better appearing

that we can not simply replace a sigmoid of large parameter with Heaviside function. The meaning of "large" for validity of this replacement, much depends on the context of the problem.

4 Traveling fronts

The neural information and activities are propagated by the mechanism of sequential activation of neighboring neurons. This process has been reported experimentally by in vitro and in vivo recordings [19,27]. In order to study the mechanism of neural propagating activity theoretically, these equations was applied and existence of the traveling front solutions have been investigated [5,28]. In this section, we apply the model (7) to investigate the effect of learning process (plasticity) on the traveling front shapes and speed for a network in which the synaptic weight connections are nonnegative (i.e., an excitatory network).

4.1 Existence

If we consider the change of variables $z = x - ct$ and $u(x,t) = U(z)$, we have,

$$-c\tau\partial_z U = -U + \int_{\mathbb{R}} w(z+ct, y+ct, t) f(U(y))\,\mathrm{d}y,$$
$$w(z+ct, y+ct, t) = w_m(z-y) \times \left(1 - \kappa \exp\left(-\gamma \int_0^{\delta} f(U(z+cs)) f(U(y+cs))\,\mathrm{d}s\right)\right).$$

Because of translation invariance of (7), we can assume that this solution satisfies $U(0) = h$ and $U(z) > h$ for $z < 0$, and $U(z) < h$ for $z > 0$. Furthermore, we consider the firing rate function $f(u) = H(u-h)$. Hence, for $c > 0$ we have

$$-c\tau\partial_z U + U = \int_{-\infty}^{0} w_m(z-y) \times \left(1 - \kappa \exp\left(-\gamma \max\left\{0, \min\left\{-\frac{z}{c}, -\frac{y}{c}, \delta\right\}\right\}\right)\right) \mathrm{d}y. \tag{19}$$

We show the right-hand side of the above relation by $F(z)$. Since F is bounded, (19) has the following bounded solution

$$U(z) = \int_0^{\infty} \mathrm{e}^{-v} F(z + c\tau v)\,\mathrm{d}v. \tag{20}$$

For $z > 0$, we have

$$F(z) = (1-\kappa)\int_{-\infty}^{0} w_m(z-y)\,\mathrm{d}y,$$

so

$$U(z) = (1-\kappa)\int_0^{\infty}\int_{z+c\tau v}^{\infty} \mathrm{e}^{-v} w_m(y)\,\mathrm{d}y\,\mathrm{d}v. \tag{21}$$

We conclude that,

$$\begin{aligned} h = U(0) &= (1-\kappa)\int_0^{\infty}\int_{c\tau v}^{\infty} \mathrm{e}^{-v} w_m(y)\,\mathrm{d}y\,\mathrm{d}v \\ &= (1-\kappa)\int_0^{\infty}\left(1-\mathrm{e}^{-y/c\tau}\right) w_m(y)\,\mathrm{d}y. \end{aligned} \tag{22}$$

In the case of exponential kernel $w_m(x) = \frac{1}{2}\mathrm{e}^{-|x|}$, we arrive at

$$h = \frac{1-\kappa}{2(1+c\tau)}.$$

It is noteworthing that the condition for the existence of traveling front, does not depend on the value of δ. Even its speed is independent of δ and this parameter only slightly affects the front shape.

Theorem 4 *There exists a unique traveling front for system* (7) *provided that* $h < (1-\kappa)\int_0^{\infty} w_m(y)\,\mathrm{d}y$.

Proof We show that for a value of c, the relation (22) is valid. Trivially, its right-hand side is decreasing with respect to c and it converges to zero when c approach to infinity (according to dominated convergence theorem). Also, when c approaches to zero, it will converge to $(1-\kappa)\int_0^{\infty} w_m(y)\,\mathrm{d}y$ (according to monotone convergence theorem). Hence, for some value of c, the relation (22) is valid. □

According to the relation (21) and the assumption that the synaptic weight function is nonnegative everywhere, we imply that $U(z)$ is a decreasing function for $z > 0$. Also from the fact $\lim_{z\to+\infty} F(z) = 0$ and the form of solution (20), it is obvious that $\lim_{z\to+\infty} U(z) = 0$. But if $\lim_{z\to-\infty} F(z) = F_*$ then also we have $\lim_{z\to-\infty} U(z) = F_*$ according to (20). To calculate F_*, note that,

$$\begin{aligned} \lim_{z\to-\infty} F(z) &= \lim_{z\to-\infty}\int_{-\infty}^{0} w_m(z-y) \\ &\quad\times\left(1-\kappa\exp\left(-\gamma\max\left\{0,\min\left\{-c^{-1}y,\delta\right\}\right\}\right)\right)\mathrm{d}y \\ &= \lim_{z\to-\infty}\left(\int_{-\infty}^{-c\delta}\left(1-\kappa\mathrm{e}^{-\gamma\delta}\right) w_m(z-y)\,\mathrm{d}y\right. \\ &\quad\left.+\int_{-c\delta}^{0}\left(1-\kappa\mathrm{e}^{\gamma c^{-1}y}\right) w_m(z-y)\,\mathrm{d}y\right) \\ &= \left(1-\kappa\mathrm{e}^{-\gamma\delta}\right)\int_{\mathbb{R}} w_m(y)\,\mathrm{d}y. \end{aligned}$$

4.2 Stability

Let $u(x,t) = V(z,t) = V(x-ct,t)$. We rewrite the system in terms of V, and linearizing around traveling front solution $U(z)$ and letting $\sigma = |U'(0)|^{-1}$,

$$\begin{aligned} \tau V_t - c\tau V_z &= -V + \int_{\mathbb{R}} \omega(z+ct, y+ct, t) f(U(y))\,\mathrm{d}y \\ &\quad +\sigma w(z+ct, ct, t) V(0,t), \\ \omega(z+ct, y+ct, t) &= \gamma\kappa\sigma w_m(z-y)c^{-1}\exp \\ &\quad\times\left(-\gamma\int_0^{\delta} f(U(z+cs))f(U(y+cs))\,\mathrm{d}s\right) \\ &\quad\times\int_0^{\delta}\left(f'(U(z+cs))f(U(y+cs))V(z+cs,t-s)\right. \\ &\quad\left.+f(U(z+cs))f'(U(y+cs))V(y+cs,t-s)\right)\mathrm{d}s. \end{aligned}$$

Hence,

$$\begin{aligned} \tau V_t &= c\tau V_z - V + \sigma(1-\kappa) w_m(z) V(0,t) \\ &\quad + \int_{-\infty}^{0} \omega(z+ct, y+ct, t)\,\mathrm{d}y. \end{aligned}$$

By substituting $V(z,t) = e^{\lambda t} V(z)$, the eigenvalue equation is obtained,

$$\tau\lambda V = c\tau V_z - V + \sigma(1-\kappa) w_m(z) V(0) + \int_{-\infty}^{0} g(z,y)\,\mathrm{d}y,$$

where,

$$\begin{aligned} g(z,y) &= w_m(z-y)\gamma\kappa\sigma c^{-1}\exp \\ &\quad\times\left(-\gamma\int_0^{\delta} f(U(z+cs))f(U(y+cs))\,\mathrm{d}s\right) \\ &\quad\times\int_0^{\delta}\left(f'(U(z+cs))f(U(y+cs))V(z+cs)\right. \\ &\quad\left.+f(U(z+cs))f'(U(y+cs))V(y+cs)\right)\mathrm{e}^{-\lambda s}\,\mathrm{d}s. \end{aligned}$$

For $z > 0$, we have $g(z,y) = 0$, so

$$(\lambda+1)V = cV_z + \sigma(1-\kappa) w_m(z) V(0),$$

so for $\mathrm{Re}\lambda + 1 > 0$,

$$\begin{aligned} &\exp(-c^{-1}(\lambda+1)z)V(z) \\ &= \sigma(1-\kappa)c^{-1}V(0)\int_z^{\infty}\exp(-c^{-1}(\lambda+1)y) w_m(y)\,\mathrm{d}y. \end{aligned}$$

and by tending $z \to 0$ from above, we can obtain in this case,

$$1 = \sigma(1-\kappa)c^{-1}\int_0^\infty \exp(-c^{-1}(\lambda+1)y)w_m(y)\,\mathrm{d}y.$$

But this equation is true only at $\lambda = 0$ because of the definition of σ which shows that the traveling front is always stable.

5 Conclusion

In this paper, a new learning dynamics for continuous neural network is derived and its effect on various types of bump solutions is discussed. The new rule is based on correlated activity much as the familiar Hebbian type of learning and satisfies the major biological constraint of synaptic boundedness. An interesting feature of our proposed rule is that changes in synaptic strength depends on changes of correlated activity in a specified time window.Importantly, present activity as compared to past correlated activity in a prescribed time window will have a differing effect on synaptic weight as determined by Eq. (6): An increase in correlated activity strengthens the synaptic weight where as a decrease in activity will have the opposite effect. A major observation of the present study is to show that restriction to a specific time window will transform the existing continuous network to a delay type of rate model for which some partial analytical results are obtained. An interesting question would then be as to how variations in the given parameter specifying the limited time window changes the network properties related to the existence and stability of the bump solutions. Indeed, modulating the time window of working memory in neural population may very much depend on the changing dynamics of such a parameter. In general, how a complex system, such as the brain, may control the parameters related to the wide range of dynamics underlying diverse memory tasks is very much unknown. It is known for example that memory for the shape of objects may endure longer than memory of the object's color, perhaps due to the less significant information conveyed by color compared to the shape of an object [8]. This could well be modulated by a mechanism where the gain of correlated activity is controlled by the duration of the time window δ, depending on the context and state of the system at a given time. This raises the interesting question of how the parameter δ plays a role as bifurcating parameter in controlling the changing dynamics of bump and traveling wave solutions obtained in the present work.

Here we briefly state the main results of this manuscript. First of all, we must mention that in our results, the parameters δ, the delay parameter, and γ, the speed of learning, does not play independent roles and they appear only as they product, $\gamma\delta$. Henceforth, we may ignore the speed of learning by modulating the time window length.

The existence as well as the stability of the prevailing solutions of the network, which are rest-state, one-bump and traveling front solutions, and their dependency on the delay parameter are investigated. In the resting state, which a complex system such as a brain favorably requires to be in the absence of external stimulus, it has been shown that the system becomes stable (i.e., preserves its uniform activity) if it possesses small and large values of time delay δ; however, it loses stability for an intermediate range. For the one-bump solutions which are known as possible stable memories of the system, the network can have a wider range of bump widths with respect to those found in the classic neural fields. Additionally, for small bump widths, bumps can be maintained if the synaptic weights of the network have the ability to take the recent neural activities into account. So by changing the time window, a network can keep its memories which may be lost for the networks that are not benefited from such efficacy dynamics. For the case of traveling front the time window length δ has no effect on the existence and stability of this type of solution and corresponding speed, but it only slightly affects the front shape.

Another worth-mentioning fact is the sensitivity of some results to the sigmoid parameter β, especially in the stability of rest states and bumps, as one can see in Fig. 2 and other simulations.

There are at least three main directions toward which the present work may be continued. First of all, investigating the well-posedness of the problem especially with respect to the nonlinearity of the gain function employed in the original system is an interesting and perhaps a difficult mathematical subject to pursue. In yet another direction, one may consider other types of Hebbian learning including delay and some variants of anti-Hebbian type of learning, ours' being the simplest choice of learning in the context of a simple neural field equation. Finally, extending the results in the case of a two-dimensional neural field is perhaps most relevant to what is now an active research area in models of working memory and activity propagation in the brain.

Acknowledgments It is pleasure for the authors to thank A. Abbasian for his useful comments about the biological aspects of the problem. This research was in part supported by a grant from IPM (No. 91920410). The third author was also partially supported by National Elites Foundation.

Appendix: Proof of Theorem 1

Proof We claim that in (9), if $\mathrm{Re}\lambda \geq 0$, we must have $\mathrm{Im}\lambda = 0$. If it is not the case, assume that $\lambda = r + \mathrm{i}m$ and $m \neq 0$ and $r \geq 0$. Let $\theta = \alpha\gamma\tau^{-1} f(\overline{u})^2 f'(\overline{u})(W + \widehat{w}_m(\xi))$ and considering imaginary parts of (9),

$$m - \theta \frac{r\mathrm{e}^{-\delta r}\sin(\delta m) - m\left(1 - \mathrm{e}^{-\delta r}\cos(\delta m)\right)}{r^2 + m^2} = 0.$$

Since $m \neq 0$,

$$r^2 + m^2 = \theta\left(r\mathrm{e}^{-\delta r}\frac{\sin(\delta m)}{m} + \mathrm{e}^{-\delta r}\cos(\delta m) - 1\right).$$

Therefore we obtain

$$r^2 < \theta\left((\delta r + 1)\mathrm{e}^{-\delta r} - 1\right) \leq 0,$$

which is a contradiction (Note that $\theta \geq 0$).

The left-hand side of (9) is an increasing function of $\lambda \in [0, \infty]$. Therefore, its value at $\lambda = 0$ must be positive for stability, i.e.,

$$1 - (1-\alpha) f'(\overline{u})\widehat{w}_m(\xi) - \alpha\gamma\delta f(\overline{u})^2 f'(\overline{u})(W + \widehat{w}_m(\xi)) > 0,$$
$$\text{for every } \xi \in \mathbb{R}.$$

which concludes the results in the desired cases. (Note that $\widehat{w}_m(\xi) \leq W$ when the synaptic weight kernel is positive everywhere and also in the other case, Mexican-hat kernel $w_m(x) = \frac{1}{4}(1 - |x|)\mathrm{e}^{-|x|}$, we have $W = 0$ and $\widehat{w}_m(\xi) \leq \frac{1}{4}$). Also in the first case, $\overline{u}$ is a root of $\left(1 - \kappa\mathrm{e}^{-\gamma\delta f(\overline{u})^2}\right) W f(\overline{u}) - \overline{u}$ and the stability condition reads that the derivative of this function with respect to $\overline{u}$ should be negative at $\overline{u}$ and this is the case for the extreme possible values of $\overline{u}$ (which are of course positive) since the value of this function is positive at zero and negative at infinity. In fact in general, the possible constant steady states are alternatively stable and unstable. □

References

1. Abbott LF, Nelson SB (2000) Synaptic plasticity: taming the beast. Nat Neurosci 3:1178–1183
2. Amari S (1977) Dynamics of pattern formation in lateral-inhibition type neural fields. Biol Cybern 27:77–87
3. Baladron J, Fasoli D, Faugeras OD, Touboul J (2011) Mean field description of and propagation of chaos in recurrent multipopulation networks of Hodgkin–Huxley and Fitzhugh–Nagumo neurons. arXiv:1110.4294
4. Bienenstock EL, Cooper LN, Munro PW (1982) Theory for the development of neuron selectivity: orientation specificity and binocular interaction in visual cortex J Neurosci 2:32–48
5. Bressloff PC (2009) Lectures in mathematical neuroscience. Mathematical biology, IAS/Park City mathematical series 14, pp 293–398
6. Bressloff PC (2012) Spatiotemporal dynamics of continuum neural fields. J Phys A Math Theor 45(3):033001
7. Bressloff PC, Coombes S (2013) Neural bubble dynamics revisited. Cogn Comput 5:281–294
8. Connell L (2007) Representing object colour in language comprehension. Cognition 102(3):476–485
9. Coombes H, Schmidt S, Bojak I (2012) Interface dynamics in planar neural field models. J Math Neurosci 2(1):1–27
10. Coombes P, Beim Graben S, Potthast R (2012b) Tutorial on neural field theory. Springer, Berlin
11. Coombes S (2005) Waves, bumps, and patterns in neural field theories. Biol Cybern 93:91–108
12. Coombes S, Owen MR (2007) Exotic dynamics in a firing rate model of neural tissue with threshold accommodation. In: Botelho F, Hagen T, Jamison J (eds) Fluids and waves: recent trends in applied analysis, vol 440. AMS Contemporary Mathematics, pp 123–144
13. Dayan P, Abbott LF (2003) Theoretical neuroscience: computational and mathematical modeling of neural systems. J Cogn Neurosci 15(1):154–155
14. Ermentrout GB, Cowan JD (1979) A mathematical theory of visual hallucination patterns. Biol Cybern 34:137–150
15. Földiák P (1991) Learning invariance from transformation sequences. Neural Comput 3(2):194–200
16. Galtier MN, Faugeras OD, Bressloff PC (2011) Hebbian learning of recurrent connections: a geometrical perspective. Neural Comput 24(9):2346–2383
17. Gerstner W, Kistler WK (2002) Mathematical formulations of Hebbian learning. Biol Cybern 87:404–415
18. Goldman-Rakic PS (1995) Cellular basis of working memory. Neuron 14:477–485
19. Golomb D, Amitai Y (1997) Propagating neuronal discharges in neocortical slices: computational and experimental study. J Neurophysiol 78(3):1199–1211
20. Hebb DO (1949) The organization of behavior; a neuropsychological theory
21. Huang X (2004) Spiral waves in disinhibited mammalian neocortex. J Neurosci 24:9897–9902
22. Itskov D, Hansel V, Tsodyks M (2011) Short-term facilitation may stabilize parametric working memory trace. Front Comput Neurosci 5(40)
23. Lu Y, Sato Y, Amari S (2011) Traveling bumps and their collisions in a two-dimensional neural field. Neural Comput 23:1248–1260
24. Miller KD, MacKayt DJC (1994) The role of constraints in Hebbian learning. Neural Comput 6:100–126
25. Oja E (1982) Simplified neuron model as a principal component analyzer. J Math Biol 15(3):267–273
26. Olshausen BA, Field DJ (1997) Sparse coding with an overcomplete basis set: a strategy employed by v1? Vis Res 37(23):3311–3325
27. Pinto DJ (2005) Initiation, vitro involve distinct mechanisms. J Neurosci 25:8131–8140
28. Pinto DJ, Ermentrout GB (2001) Spatially structured activity in synaptically coupled neuronal networks: I. Traveling fronts and pulses. SIAM J Appl Math 62:206–225
29. Rao RPN, Sejnowski TJ (2001) Spike-timing-dependent Hebbian plasticity as temporal difference learning. Neural Comput 13(10):2221–2237
30. Robinson PA (2011) Neural field theory of synaptic plasticity. J Theor Biol 285:156–163
31. Sandstede B (2007) Evans functions and nonlinear stability of traveling waves in neuronal network models. Int J Bifurc Chaos 17:2693–2704
32. Sejnowski TJ (1977) Statistical constraints on synaptic plasticity. J Theor Biol 69(2):385–389
33. Wallis G, Baddeley R (1997) Optimal, unsupervised learning in invariant object recognition. Neural Comput 9:883–894
34. Wilson HR, Cowan JD (1972) Excitatory and inhibitory interactions in localized populations of model neurons. Biophys J 12:1–24
35. Wilson HR, Cowan JD (1973) A mathematical theory of the functional dynamics of cortical and thalamic nervous tissue. Kybernetika 13(2):55–80